Segmentation of infrared images: a new technology for early detection of breast diseases

J.P. S. de Oliveira, A. Conci,
Computer Science Dep. Computer Institute, Federal Fluminense University, UFF - CEP 24210-240, Niterói, RJ, Brazil
aconci@ic.uff.br

[a]María G. Pérez,
[a]Facultad de Ingeniería en Sistemas, Electrónica e Industrial, Universidad Técnica de Ambato - Ecuador
Cdla. Universitaria
maria.espanya@gmail.com

[a,b]Víctor H. Andaluz
[b]Universidad de las Fuerzas Armadas ESPE
Sangolquí, Ecuador
Av. General Rumiñahui
vhandaluz1@espe.edu.ec

***Abstract*-In a first stage a cancer promotes an intense process of vascularization at the affected area increasing blood flow and modifying the local temperature of the body. Using a thermal camera, the infrared radiation emitted by the human body can be captured and then used in the measuring of body temperature, turning the results into an image. Moreover, thermography can detect suspicious regions in patients of any age, even in cases of dense breasts, where the detection of an abnormality cannot be accomplished by others exams. A fundamental step in the use of thermal images is the development of computer aided diagnosis (CAD) systems. These could allow the execution of exams by technicians, following well established routines and protocols, as already occurs in mammography exams, allowing doctors to have a greater possibility of dedication in the analysis and in the meaning of the exams. In this work, an automatic detection of the regions of interest (ROI) is proposed and compared with segmentations performed manually. This work presents a methodology for the automatic segmentation of lateral breast thermal images. For the evaluation of the results, different groups of ground truth are generated, which are available on the internet, in order to allow the verification of the results' correctness. Finally, the obtained results by the proposed methodology for the 328 images used in this work are demonstrated. The results showed average values of accuracy**

Keywords— Image Processing; Termography; Breast Cancer; Computer aided diagnosis (CAD) systems; Region of Interest (ROI), Dense Breast; Infrared Radiation body; Early Detection, corner; segmentation.

I. INTRODUCTION

Cancer is the leading cause of death worldwide [1, 2]. Cancer mortality can be reduced if are detected and treated early. Every year, more than 20% of newly diagnosed cases are related to breasts, establishing breast cancer as the major cause of cancer deaths in females. The early detection activities have two components: early diagnosis and screening [3]. However, any development towards a CAD system or even an exam guided by a computer should consider a suitable extraction of the region of interest (ROI). The World Health Organization estimates that annually arise over 1 million new cases and has caused more than 458,000 deaths in the world. In 2004; 519,000 women died from this cause across the globe, with this total 69% in developing countries [4]. According to statistics from the National Cancer Institute [1], in 2012 are expected 52,680 new cases of breast cancer, with an estimated risk of 52 cases per 100 thousand women: in Brazil [5]. Detection of breast cancer at early stages would increase by 85% the chances of cure, whereas when the disease is detected in advanced stages, this percentage is reduced to 10% [6]. After five years of diagnosis, the median survival of patients in developed countries is 85%, while in developing countries reach only 60%, on average [1, 5].

This paper proposes a methodology for the automatic segmentation of lateral thermal breast imaging. Some previous work on extracting ROI thermal imaging breast and pattern generating segmentations (ground truth) is discussed. An automatic methodology consists of various image processing techniques, such as threshold, clustering, detection and refinement of corners. To validate the results, we have generated segmentations group patterns available on the internet so that proper verification of the results is possible. Finally, the results obtained by the method proposed for the case of 328 lateral images used in the experiments are shown. These results present mean values of accuracy and sensitivity of 96% and 97% respectively.

II. BREAST CANCER

Breast cancer was by far the most common cancer diagnosed in women (25.2% of all new cases in women) [7]. Table I shown the rate the incidence by breast cancer in women considering at north, south, central, west and eastern of European countries, as well as at United State, Canada, Brazil, Latin American and, Caribbean and Ecuador, standardized rate per 100,000.

TABLE I. RATES OF INCIDENCE BREAST CANCER [8]

Region/country	Incidence
Europe (north)	128,8
Europe (Central and East)	63,4
Europe (South)	97,8
Europe (West)	134,3
United State	143,8
Canada	124
Latin American and Caribbean	549,3
Brazil	50,7
Ecuador	31,772

A. Mortality from breast cancer

The most widely used early detection of tumors are the clinical breast exam, self-examination, ultrasonography, MRI and mammography [9, 10]. The mammography is the main tool for diagnosing breast cancer, and is regarded as the gold standard [11] in early detection. However, mammography has

significant disadvantages as the cumulative ionizing radiation, can be carcinogenic. Other disadvantages of mammography are the pain caused by compression of the breast during the examination, the high cost (compared to thermography, for example), the difficulty in identifying malignancies in denser (in young women) breasts, among other factors. More information about the causes, types, origins and definitions of cancer in general and breast cancer, or to inquire about the various types of tests for the early detection of breast tumors can be found in [1,5,10,12-17].

III. Medical Thermography

Since its appearance 30 years ago, thermography has undergone several medical studies to investigate its efficiency as a low-cost, non-invasive [18]. In a thermal image, characteristic changes of temperature patterns in normal image can be associated with different types of diseases. From the analysis of these changes non-invasive investigation to assist in the diagnosis of possible diseases [18]. Thermography is a method of image capture relatively simple, fast, inexpensive, painless the surface temperature of the body, taking a measurement of infrared radiation emitted [9, 19]. Additionally, thermography provides functional information, with the ability to detect physiological response of tissue, not only the anatomical features [11, 20]. Because of its ability to provide information on physiological changes of human skin, thermography can be used for early detection of tumor formation in the breast, even prior, such as mammographies [21, 22]. The combination of clinical examination, mammography and thermography can set the sensitivity of early detection of breast cancer in 98% of cases [23]. Fig. 1 shows two thermal breast imaging at different positions. The lateral position is the object of our study. Additional information on Medical Thermography can be found in [10, 14, 15, 17, 24, 25].

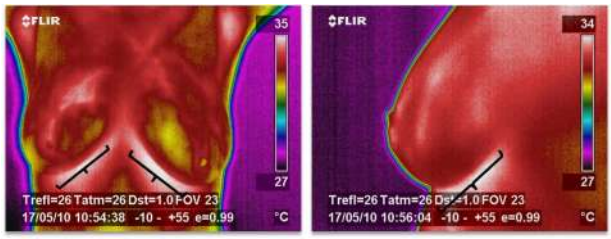

Fig. 1. High temperatures in the inframammary fold region

A new project to acquire breast thermal imaging under development by Hospital Universitario Antonio Pedro (HUAP) was approved by the Ethics Committee of the Ministry of Health on June 6, 2012. In this work we have studied and experimented a new imaging protocol currently used in the acquisitions in the HUAP, whose aim is to acquire thermal images of up to two thousand volunteer. This uses a thermal camera FLIR ThermaCAM.

IV. Material and Method Proposed

In literature, many author presented a methods to segment the thermograms and to detect regions of potentially suspicious tissues from breast thermograms [26-28]. Acharya et al. [29] used texture features and SVM classifier to detect signs of breast cancer. Misolenic et al. [22] presented a method to segment thermograms and extract suspected hot regions from the background. Kolestani et al [30] proposed three different segmentation algorithms: K-means, fuzzy, c-means and level set, by which detected the hottest regions on three different approaches for each case are extracted and compared, Suganthi and Ramakrshhan [31] used Level Set Method. Duarte et al.[32] proposed thermographic processing software allows the user to select any ROI independently of its geometric shape. It also contains a segmentation algorithms based on the thresholding as a segmentation method. The segmentation algorithm optimizes the chosen region by removing areas that don´t have any relevant statistic data in order to take into account only the temperature of the ROI that will be used in further characterization. [33]. W. Jamrozik [33] proposed a segmentation method using supervised approach based on a cellular neural networks is presented. Simulated annealing and genetic algorithm were used for training of the network (template optimization). Comparison of proposed method to a well elaborated segmentation method based on region growing approach was made. Obtained results prove that the cellular neural network can be a valuable tool for infrared welding pool images segmentation. Araujo et al. [34], performed a process for the breast segmentation ellipsoidal elements for selecting the whole area of each breasts. At this point, ellipses were adjusted for the patient's breasts. In Machado et al. [35], a segmentation method based in topological diferencial was used. In [14], Otsu method and Laplacian filters were used for lateral and upper segmentation, thresholding, region growing and clustering techniques to detect the lower breast boundaries and uniform quadratic basis splines was used to smooth the initial set points. Mota et al. [36] proposed a segmentation method with several steps involved. In this work, the proposed method aims at guiding, automatically, the region of interest (ROI) in thermal imaging breast side. The proposed method consists of two main steps, which are subdivided into several sub-steps: remove the background image and the segmentation of the region of interest. Fig. 2 shows the substeps used in the extraction of the ROI of IR_4892 image. The thermal image in shades of gray is shown in Fig. 2 (a). In Fig. 2(b) and (c) the results of thresholding process and the process of clustering of the image, respectively, are shown. In Fig. 2 (d) the corners of the image obtained after the detection and refinement processes are shown. Finally (e) shows the segmented image.

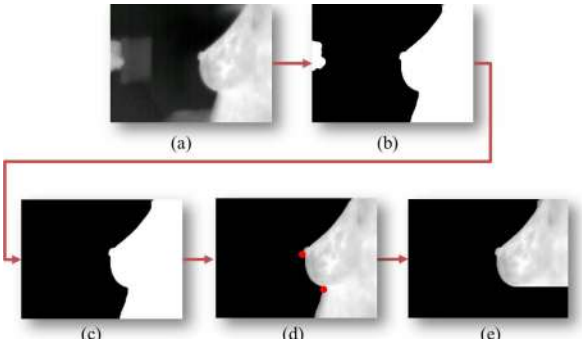

Fig. 2: Substeps of the proposed method: (a) the thermal image. (b) Threshold, (c) Removal of unwanted elements. (d) Detection and refinement of corners and (e) the final segmentation.

Next we present an overview of the proposed method. A description of the two types of thermal imagers. The first step of the method is described in subsequent section, which handles all processing of the image before applying, *i.e.,* background suppression and removal of undesirable elements. As well as the general definition of the corner detection. Then, the method of Shi-Tomasi, used in this work, and all its features are presented. Finally, some results obtained with the proposed method is presented.

A. Used Images

In this paper we Proeng [37] thermal images captured at eight different positions in relation to the camera. For the breast side ROI tests in this work 180 images of two specific positions adquired with a viewing angle perpendicular to sagittal plane. The proposed method is also applied to the captured images the new UFF acquisition protocol. Images used to draw the region of interest were obtained with FLIR Therma CAM S45 camera, capable of obtaining measurements without contact. Fig. 3 shows the image UFPE database. Initially, the pre-processing stage is performed to transform all thermal images shades of gray (Grey palette) using FLIR Quick Report 1.2 software [38]. These conversion processes are described in [15], generate a copy of the resulting image in bitmap format.

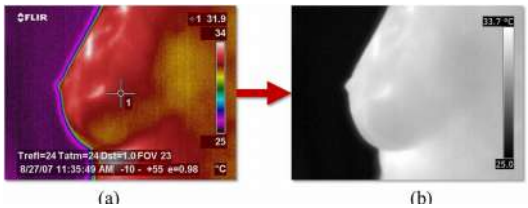

Fig. 3: Typical image of two palettes: (a) Rain Palette. (b) Grey Palette

According Motta [15], such a transformation is necessary because the images in gray level are preferred by radiologists, as they have a greater similarity to the images of the mammographic examinations. Therefore, through their matrices temperatures each image is represented by means of pseudo colors available by the software of the thermal FLIR, corresponding to 120 of gray, ranging from 0 (black), lower temperature to 255 (white).

B. Remove the background

After the initial stage of conversion, images pass through a processing stage, the aim is to perform a complete removal of the background, leaving only the patient's body. This step consists of image using the threshold and the elimination of undesirable elements in the region of interest.

C. Thresholding

Following the procedure adopted by Marques [14], the histograms of some of the thermal images available on databases to assess the feasibility of the methods of the threshold is performed. For analysis of these histograms, it can use a common pattern of bimodal images: a fashion that represents the background image and another that represents the body of the patient [39], [40], [41] and [42].

Fig. 4 shows some typical histograms for images IR_0108, IR_0111, IR_0209, IR_0214, IR_0624, IR_0832, IR_0961, IR_0974 and IR_1725. In all these graphs the horizontal axis represents the gray level from 0 to 255 and the vertical axis the number of pixels in the image with the respective level. A clear division of the histogram into two classes (or two modes) facilitates the choice of method for balancing the histogram [43]. The aim of this method is to find the ideal gray level to divide the histogram into two distinct classes. So that, at each iteration, the method performs the weighting of the histogram of the image in order to check which side is the heaviest. Thus, the method removes the weight progressively until the two sides are balanced. Pixels greater than the threshold are converted to white, while the others become black.

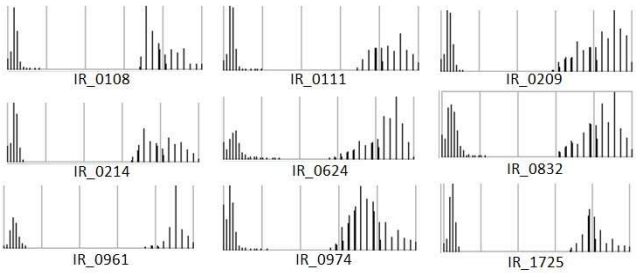

Fig. 4: Histograms of some thermal images used

The whole process is specified in Fig. 5, where the numbers indicate the execution steps of the method and the white color indicates the removed weights lighter side histogram at each iteration. The latest iteration of the method, indicated when both sides are in balance, obtaining a threshold regarding the final value of the midpoint of the balanced histogram.

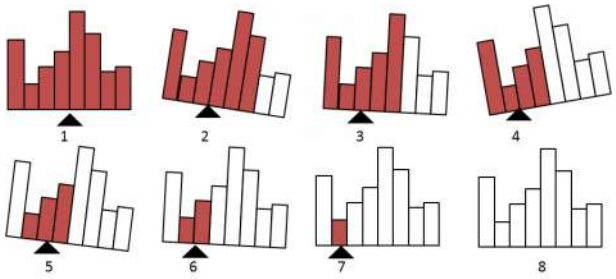

Fig. 5: Stages of histogram thresholding for balance, adapted from [44].

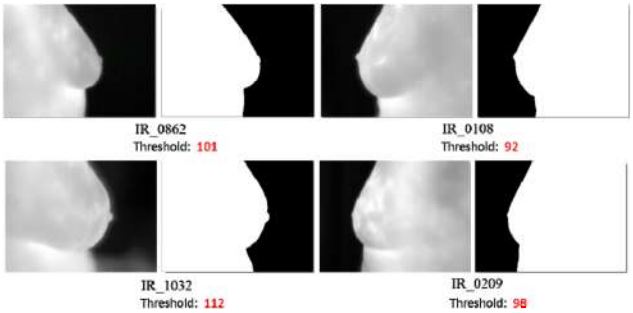

Fig. 6: Original and the background images removed by thresholding

Fig. 6 shows four images of the UFPE database IR_0862, IR_0108, IR_1032 and IR_0209 and by the histogram

equilibrium. As the threshold value is calculated from the histogram of each image, the method operates adaptively to the characteristics of the different images.

D. *Removing unwanted items*

At the time of capture images, unwanted elements can be included in images, from external factors and are not completely removed by the thresholding process.

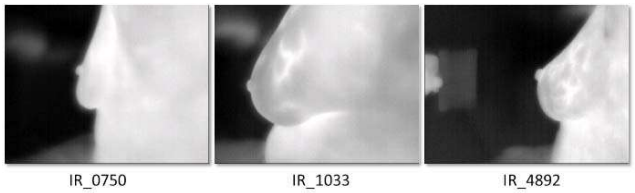

Fig. 7: Images unwanted items in the background

A proposal to remove unwanted elements is clusters according to the neighborhood and likeness.

Given a set with n elements $X = \{X_1, X_2, ..., X_n\}$ one clustering involves obtaining a set of k clusters, $C = \{C_1, C_2, ..., C_k\}$, such that there is more similarity between content items in a cluster than any of these elements with a set of other C [45], as shown in Fig. 8.

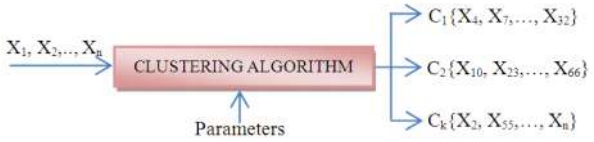

Fig. 8: Functional scheme of clustering algorithm. Adapted of [45].

The set C is considered a clustering with k clusters, if the following conditions are satisfied:

$$\begin{aligned} &\cup_{i=1}^{k} C_i = X \\ &C_i \neq 0 \ \text{ para } 1 \leq i \leq k \\ &C_i \cap C_j = 0 \text{ para } 1 \leq_i, \ j \leq k, i \neq j \end{aligned} \tag{1}$$

For this work, each group is responsible for grouping neighboring pixels that are similar and different from others [46]. Therefore, clusters divide the image so that the data become more discerning and easy to use

As shown in Fig. 7, there are two distinct groups in the images: the background and the patient's body. Therefore, clustering method is proposed in this paper, it does a complete verification of the neighborhoods and creates two groups; the body always has a higher number of pixels that the element cluster spam. Therefore, the larger and the lower group is removed. After removing the background, the image is subdivided into two groups. The smallest amount of unwanted items, it is removed (see figure 9).

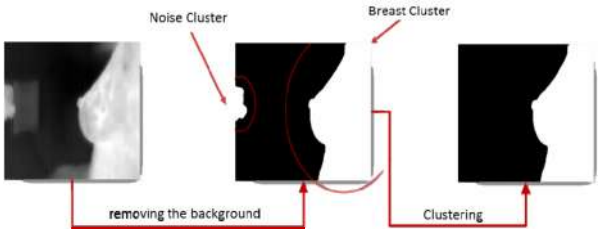

Fig. 9: Thresholding process

E. *Segmentation of the region of interest*

1) The segmentation process is divided into three main stages: the detection of the corners of the image, Shi-Tomasi method and obtaining the segmented image.

a) Detection of corners

On an image, a corner is set to a point that there are two dominant and distinctive addresses in the local vicinity to this point edges. An image gradient, given by Equation 2, measures the change in this type of image. Two parameters of information are provided by the gradient: their magnitude, which represents the variation in speed of an image, and the direction of the set of gradients, which indicate in which direction the image is varying [49].

$$\nabla f(x,y) = \frac{\partial f}{\partial x} + \frac{\partial f}{\partial y} \tag{2}$$

Therefore, a corner characterized by a region of intersection of two edges, that is, a point in an image in which there is a considerable change in intensity (gradient) in the vertical direction and the horizontal direction.

Figs 10, 11 and 12 show three possible types of variable intensity in small windows on a generic image and a thermal image side of the breast. In the image shown in Fig 10, there is no significant change in intensity in any direction. Therefore, with respect to the goal of this paper, there is not information relevant to consider in the image.

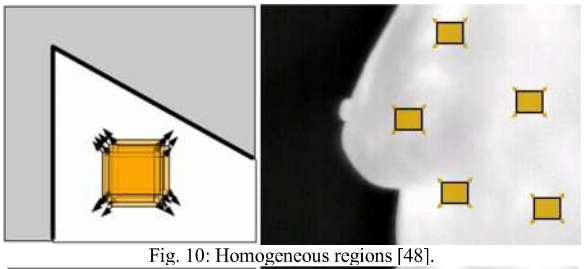

Fig. 10: Homogeneous regions [48].

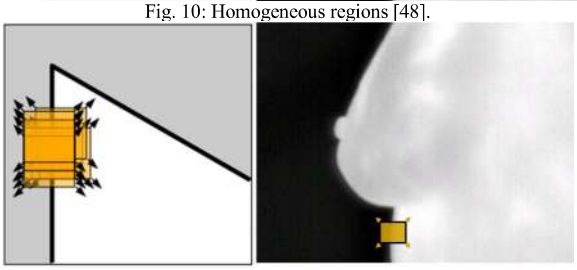

Fig. 11: Behavior in an edge [48]*

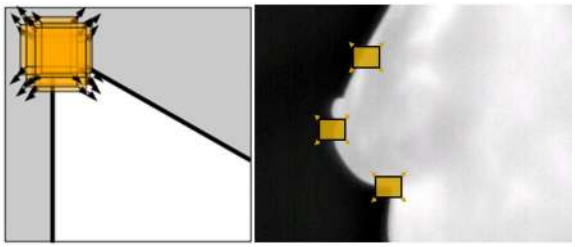

Fig. 12: Behavior in a corner [48]

In Fig. 11, the intensity variation occurs in a direction parallel to the contour of the trunk of the patient corresponding to the image, which characterizes the presence of an edge. In Fig. 12, a significant change is observed in two directions, defining the presence of corners in several points of the contour of the breast. In this picture, you can check corners in regions like the inframammary fold, the region of the areola and the upper limit of the breast.

b) Theoretical foundation

Let (x, y) be the origin of any ROI of image and let (u, v) he shifted region. Considering I(x,y) an intensity image in any position, the sum of squared differences between I in a region R (u, v), denoted by S, is given by equation 3:

$$S(u,v) = \sum_x \sum_y w(x,y)\,[I(x+u, y+v) - I(x,y)]^2 \quad (3)$$

Where S represents the difference between the original image and a shifted window [49]. The displacements of the window the directions x and y are given by u and v, respectively. w (x, y) defines an window of image, whose value is equal to 1 within the window, and 0 outside the window.Whereas I_x and I_y are the partial derivatives $\frac{dI}{dx}$ e $\frac{dI}{dy}$ of I, the expression $I(x+u, y+v)$ can be approximated by Taylor series expansion to second order, generating the equation 4.

$$S(u,v) \approx \sum_x \sum_y [I(x+y) + I_x u + I_y v) - I(x,y)]^2 \quad (4)$$

Since the values of I (x, y) are canceled, the result of the power of two of the equation 4, generates the equation 5:

$$S(u,v) \approx \sum_x \sum_y u^2 I_x^2 + 2uv\, I_x I_y + v^2 I_y^2 \quad (5)$$

Rewriting equation 5 in matrix form, we have:

$$S(u,v) \approx [u,v] \left(\sum \begin{bmatrix} I_x^2 & I_x I_y \\ I_x I_y & I_y^2 \end{bmatrix} \right) \begin{bmatrix} u \\ v \end{bmatrix} \quad (6)$$

Renaming equation 6 for M and considering a window u (x, y), equation 7:

$$M = \sum_{x,y} w(x,y) \begin{bmatrix} I_x^2 & I_x I_y \\ I_x I_y & I_x^2 \end{bmatrix} \quad (7)$$

c) Analyzing the eigenvalues

The matrix M in equation 7 is defined as an array of variations of the image gradient, and M is the function of the ellipse E, located in the origin of coordinates, given by equation 8. Such an ellipse provide intensity variations along the directions of the image [50, 49].

$$E = \begin{bmatrix} \sum I_x^2 & \sum I_x I_y \\ \sum I_x I_y & \sum I_y^2 \end{bmatrix} \quad (8)$$

The distribution of the derivatives of x and y vary according to the directions of intensity of the image and can be characterized by the shape and the size of the principal components of the ellipse [50].

If the case that ellipse is defined as equation 8, the gradient directions are aligned with the x-axis with the y axis. If the eigenvalues, λ_1 and λ_2, were close to zero, the point under analysis is not a corner. As the eigenvectors define the directions of the edges, while the definition of the eigenvalues represents their magnitude, it can be concluded that a corner should be located in a region in which the smallest eigenvalue is found [50]. If an area presents a region of constant intensity, the two eigenvalues are small and close to zero. Therefore, if $\lambda_1 \approx 0$ and $\lambda_2 \approx 0$, the pixel (x, y) has no information related to the intensity [51].

2) Detection of corners by Shi-Tomasi method

The corner detector proposed by Shi and Tomasi [52] tire locates the most prominent corners in an image or a specific region of an image and is based entirely on the Harris corner detector [51], as well except allow selecting corners [49]. A rank value is calculated for each pixel, and if this value is below a certain threshold, the pixel in question is defined as a corner. The values of λ_1 and λ_2 are used to determine the presence or absence of edges in the image (Fig. 13) [53]. In the Harris detector, classification is the value obtained by R, given by Equation 9 the Shi-Tomasi method, only the eigenvalues λ_1 and λ_2 are considered. Thus R is given by:

$$R = \min(\lambda_1, \lambda_2) \quad (9)$$

Fig. 13 shows the classification the region of an image according to the eigenvalues [51]. The regions in green, pink and blue and gray in Fig. 13 correspond, respectively, to the regions in white (corner), red (edge) and blue (homogeneous region). In the green region the λ_1 and λ_2 are larger than a certain value, that is, a region in which pixels are considered corners; Blue and gray, or λ_1 and λ_2 is less than a defined minimum value; In pink regions both λ_1 regions represents area where and λ_2 are much smaller than a defined minimum value.

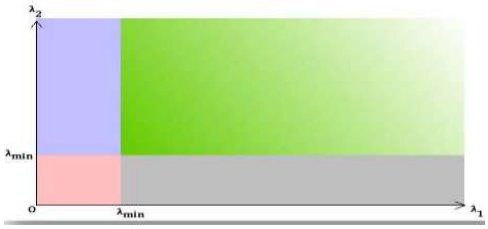

Fig. 13: Type detection according to the obtained values λ1 and λ_2 [49].

a) Steps of Shi-Tomasi method

The proposed method consists of seven steps [49].

1. Initially, the algorithm evaluates each pixel of the image by calculating the minimum eigenvalue of the gradient matrix defined in equation 7, i.e., for each pixel of the image I is obtained the minimum eigenvalue λ_m.

2. Among all the eigenvalues obtained for each pixel x, the largest eigenvalue is calculated (λ_{max}).
3. A parameter (levelOfQuality) is defined to control the quality of the obtained corners. The value is multiplied by the measurement of the corner of lower quality (λ_{max}). The result of this multiplication is a threshold (λ_{min}) used to determine if a pixel is a corner or not:

$$\lambda_{min} = \text{levelOfQuality} * \lambda_{max} \quad (10)$$

The corners measure below this threshold are rejected

4. Pixels whose eigenvalues are less than a threshold are added to a list of potential corners, denoted by L. For each pixel p (x, y) of an image I:
If λ_m of p (x, y)> λ_{min} then p (x, y) is added to L
If λ_m of p (x, y) ≤ λ_{min} then p (x, y) is not added to L.

5. Corners list L is decreasingly ordered, based on the value of each pixel of λ_m.
6. After obtaining the gradients of the image, the algorithm performs maximum suppression, which is a search carried out to determine whether a gradient magnitude assumes a local maximum value in the gradient direction [54]. Therefore, in a 3x3 neighborhood, local maxima are removed
7. Finally, a threshold is defined to control the minimum distance between two potential corners. If this distance is less than minDistance, the algorithm removes from the list L the corner with smaller value of λ_m.

In Fig. 14 shows the five Corners obtained by applying this method in images IR_1747, IR_0807 and IR_5778 of UFPE database [37].

Fig. 14: Corners detected by the method Shi-Tomasi

Furthermore, to optimize the detection of corners in this paper we propose a refining step in order to get a better fit of the corners in the contour image; more specifically an adjustment related to the inframammary fold and nipple region by applying the proposed cornerSubPix [55] method [53]. The extraction process of the region of interest ends when the final segmentation of the image of the breast [53] is obtained.

V. CONCLUSION

A new methodology for the automatic segmentation of thermal images was proposed lateral breast. Using image processing techniques such as histogram threshold for balancing, clustering, detection and refinement of corners and making the extraction of the region of interest ROI from images captured in lateral positions shown in Fig. 1. This process is very important for studies and analysis of thermal images of the breast, including serving as a tool for helping medical diagnosis of diseases of the breast, such as breast cancer.

Some contributions provided by this work is to describe and discuss the will of image acquisition protocols found in the literature, beyond the static protocol UFPE applied for obtaining images of the databases used in this work. Another description provided considers the new dynamic protocol that is currently being used for thermal imaging in breast at University Hospital Antonio Pedro of UFF and the construction of the new database, which is partially used in this work. All regions of interest extracted from the thermal images used in this work and all of its standard segmentations generated Proeng are available in [37]. Thus, further studies, analyzes, comparisons and improvements in the method in order to progressively enhance the process of automatic segmentation of lateral thermal breast imaging can be performed.

ACKNOWLEDGMENT

Brazilians authors thank the institutional support provided by INCT- MACC (National Institute of Science and Technology) and the Brazilian agency CNPq. The authors from Ecuador thank the UTA and DIDE for founding the research project CU-2340-P-2013.

REFERENCES

[1] INCA. Instituto Nacional de Câncer. http://www2.inca.gov.br, 2012.

[2] GLOBALCAN, IARC. Available on: http://globocan.iarc.fr/Pages/fact_sheets_cancer.aspx, 2012.

[3] Cancer, Fact sheet no. 297. Accessed 10/16/2014. Available on: http://www.who.int/mediacentre/factsheets/fs297/es/, 2014.

[4] WHO. World Health Organization-Breast Cancer Awareness Month in October http://www.who.int/cancer/events/breast_cancer_month/en/, 2012.

[5] INCA. Instituto Nacional de Câncer-Estimativa 2012: Incidência de Câncer no Brasil. http://www1.inca.gov.br/estimativa/2012/estimativa20122111.pdf, 2012.

[6] E. Y. K. Ng, N. M. Sudharsan, Numerical computation as a tool to aid thermographic interpretation. *Journal of Medical Engineering and Technology*. vol. 25, pp. 53-60, 2001.

[7] J. Ferlay, I. Soerjomataram, M. Ervik, R. Dikshit, S. Eser, C. Mathers, M. Rebelo, DM. Parkin, D. Forman, F. Bray. GLOBOCAN 2012 v1.0, Cancer Incidence and Mortality Worldwide: IARC Cancer Base no. 11 [Online]. Lyon, France: International Agency for Research on Cancer; 2013. Available from: http://globocan.iarc.fr

[8] A. Ramalho, Instituto Nacional do Câncer: O Câncer de Mama no Brasil-Situação epidemiológica e rastreamento. Available on: http://bvsms.saude.gov.br/bvs/palestras/cancer/cancer_mama_brasil.pdf, 2009.

[9] J. Koay, C. Herry, M. Frize. Analysis of breast thermography with an artificial neural network. *Proceedings of the 26th Annual International Conference of the IEEE Engineering in Medicine & Biology Society*. vol. 2, pp. 1159-62, 2004.

[10] R. Resmini. Análise de imagens térmicas da mama usando descritores de textura. Dissertação de mestrado, Instituto de Computação, Universidade Federal Fluminense, Niterói, RJ, Brasil, 2011.

[11] M. M. Oliveira. Desenvolvimento de protocolo e construção de uma aparato mecânico para padronização da aquisição de imagens termográficas da mama. Dissertação de mestrado, Pós-Graduação em Engenharia Mecânica - Universidade Federal de Pernambuco, Recife, PE, Brasil, 2012.

[12] BCO. Breast Cancer Organization - Understanding Breast Cancer. [Online] Available on

http://www.breastcancer.org/symptoms/understand_bc/. Accessed November 15, 2012.

[13] L. A. Bezerra. Uso de imagens termográficas em tumores mamários para validação de simulação computacional. Dissertação de mestrado, Programa de Pós-Graduação em Engenharia Mecânica, Universidade Federal de Pernambuco, Recife, PE, Brasil, 2007.

[14] R.S. Marques. Segmentação automática das mamas em imagens térmicas. Dissertação de mestrado, Instituto de Computação, Universidade Federal Fluminense, Niterói, RJ, Brasil, 2012.

[15] L.S. Motta, Obtenção automática da região de interesse em termogramas frontais da mama para o auxílio à detecção precoce de doenças. Dissertação de mestrado, Instituto de Computação, Universidade Federal Fluminense, Niterói, RJ, Brasil, 2010.

[16] E. Y. K. Ng, Breast imaging: a survey, *World Journal of Clinical Oncology*, vol. 2, pp. 171_178, 2011

[17] S.V Silva. Reconstrução da Geometria da Mama a partir de Imagens Termográficas. Tese de doutorado, Instituto de Computação, Universidade Federal Fluminense, Niterói, RJ, Brasil, 2010.

[18] FLIR. Imagens Térmicas para Aplicações Médicas. http://www.flir.com/thermography/americas/br/content/?id=14536, 2012. Accessed November 15, 2012.

[19] E.Y.K. Ng, E.C. Kee, R. Acharya U, Advanced technique in breast thermography analysis. *Annual International Conference of the IEEE Engineering in Medicine and Biology Society*. vol. 1, pp. 710-713, 2005.

[20] J. Wang, K.J. Chang, C.Y. Chen, K.L. Chien, Y.S. Tsai, Y.M. Wu, Y.C. Teng, T. Shih. Evaluation of the diagnostic performance of infrared imaging of the breast: a preliminary study. *BioMedical Engineering Online*. vol. 9, pp. 3, 2010.

[21] E. Y. K. Ng, A review of thermography as promising non-invasive detection modality for breast tumor, *International Journal of Thermal Sciences*, vol. 48, pp. 849_859, 2009.

[22] M. Milosevic, D. Jankovic, A. Peulic, Thermography based breast cancer detection using texture features and minimum variance quantization, *EXCLI Journal*, vol. 13, pp. 1204-1215, 2014.

[23] E. Y. K. Ng, N.M. Sudharsan, Computer simulation in conjunction with medical thermography as an adjunct tool for early detection of breast cancer. *BMC Cancer*. vol. 4, pp. 17, 2004.

[24] J. Y. Massuda, M. E. B. Florence, M. L. Cintra, E. M. de Souza, O papel da neoangiogênese na progressão da ceratose solar para o carcinoma espino celular. In XVI Congresso Interno de Iniciação Científica - Faculdade de Ciências Médicas - Universidade Estadual de Campinas – UNICAMP, 2008.

[25] T.B. Borchartt, A. Conci, R.C.F. Lima, R. Resmini, A. Sanchez, Breast thermography from an image processing viewpoint: A survey, Signal Processing: *Signal and Image Processing Techniques for Detection of Breast Diseases*, vol. 93, no. 10, pp. 2785–2803, 2013.

[26] E. Y. K. Ng, Chen, LN. Ung, Computerized breast thermography: Study of image segmentation and temperature cyclic variations. *Int J Med Eng Technol.*, vol. 25, pp. 12-6, 2001.

[27] M. EtehadTavakol and E. Y. K. Ng. Breast thermography as a potential non-contact method in the early detection of cancer: a review. J Mech Biol. vol. 13, 2013.

[28] B. Sowmya and S. Bhatachaya, Color image Segmentation using fuzzy clustering techinques and competitive neuronal network. *Appl. Soft Comput.*, vol. 11, pp. 3170-8, 2011.

[29] U.R Acharya, E.Y.K. Ng, J.H. Tan, S.V. Sree, Thermography Based Breast Cancer Detection Using Texture Features and Support Vector Machine, *Journal of Medical Systems*, vol. 36, no. 3, pp. 1503-1510, 2012.

[30] N. Golestani, M EtehadTavakol, E. Y. K. Ng. Level Set Method for Segmentation of Infrared Breast Thermograms, *EXCLI Journal 2014*, vol. 13, pp. 241-251, 2014.

[31] S.S. Suganthi, S, Ramakrishnan, Anisotropic diffusion filter based edge enhancement for segmentation of breast thermogram using level sets. *Biomedical Signal Processing and Control*, vol. 10, pp. 128-136, 2014.

[32] A. Duarte, L. Carrao, M. Espanha, T. Viana, D. Freitas, P. Bartolo, P. Faria, H.A. Almeida, Segmentation Algorithms for thermal images, *Procedia Technology*, vol. 16, pp. 1560-1569, 2014. Available online at www.sciencedirect.com

[33] W. Jamrozik, Cellular neural networks for welding arc thermograms segmentation, *Infrared Physics & Technology*, vol. 66, pp. 18–28, 2014, doi:10.1016/j.infrared.2014.05.005.

[34] M.C. Araújo, R.C.F. Lima, R.M.C.R. de Souza, Interval symbolic feature extraction for thermography breast cancer detection. *Expert Systems with Applications*, vol. 41, no. 15, pp. 6728–6737, 2014.

[35] D.A. Machado, G. Giraldi, A.A. Novotny, R.S. Marques, A. Conci, Topological Derivative Applied to Automatic Segmentation of Frontal Breast Thermograms, 2013.

[36] L. Motta, A. Conci, R. Lima, E. Diniz. Automatic segmentation on thermograms in order to aid diagnosis and 2D modeling, in: Proceedings of 10th Workshop em Informática Médica, pp.1610–1619, 2010.

[37] PROENG. Image Processing and Image Analyses Applied to Mastology. http: //visual.ic.uff.br/en/proeng/, 2012.

[38] QuickReport. FLIR QuickReport - User's Manual. http://www.atecorp.com/ATECorp/media/pdfs/data-sheets/FLIR-B200-B250-T250-BCAM_Manual.pdf, 2012.

[39] I.N. Bankman, Handbook of Medical Imaging Processing and Analysis. Academic Press, San Diego, CA, USA, 2000.

[40] R.C. Gonzalez, R. E. Woods. Digital Image Processing, 3rd Edition, Prentice-Hall, Inc., Upper Saddle River, NJ, USA, 2006.

[41] M. McDonough, R. Bowen. Explaining Bimodal Histograms. http://www.brighthubpm.com/software-reviews-tips/62274-explaining-bimodal-histograms/, 2012.

[42] N. Nikolaidis, I. Pitas. Digital image processing in painting restoration and archiving. In Proceedings of the IEEE International Conference on Image Processing, pp. 586-589, 2001.

[43] A. Anjos, H. Shahbazkia, Bi-level image thresholding - a fast method. In International Conference on Bio-inspired Systems and Signal Processing, pp. 70-76, 2008.

[44] Wikipedia. Balanced Histogram Thresholding. http://en.wikipedia.org/wiki/Balanced_histogram_thresholding, 2012. Accessed 30 October 2012.

[45] A. Conci, E. Azevedo, F. Leta. Computação Gráfica, V.2 - Teoria e Prática. Elsevier, Rio de Janeiro, RJ, Brasil, 2008.

[46] M. Kaya, An algorithm for image clustering and compression, *Turkish Journal of Electrical Engineering and Computer Sciences*, vol. 13, 2005.

[47] D. Jacobs. Image Gradients-Class Notes. 2005. http://www.cs.umd.edu/~djacobs/ CMSC426/ImageGradients.pdf, Accessed November 24, 2012.

[48] D.P. Huttenlocher. Corner Detection, (2008). [Online]. Available: http://www.cs.cornell.edu/courses/cs664/2008sp/handouts/664%20corner%20detection.pdf. Accessed October 28, 2012.

[49] U. Sinha. The Shi-Tomasi Corner Detector. 2010. [Online]. Available: http://www.aishack.in/2010/05/the-shi-tomasi-corner-detector/. Accessed October 28, 2012.

[50] R. Collins. Lecture 06: Harris Corner Detection. http://www.cse.psu.edu/~rcollins/CSE486/lecture06.pdf, 2008. Accessed October 28, 2012;

[51] C. Harris, M. Stephens, (1994). A combined corner and edge detector. In Proceedings of Fourth Alvey Vision Conference, pp. 147-151, 1988.

[52] J. Shi, C. Tomasi. Good features to track. IEEE Conference on Computer Vision and Pattern Recognition, pp. 593-600, 1994.

[53] J.P.S de Oliveira, Extração automática da região de Interesse em imagens térmicas Laterais da mama, Dissertação de Mestrado, 2012.

[54] J. Canny, A computational approach to edge detection. *IEEE Transactions Pattern Analysis and Machine Intelligence*, vol. 8, pp. 679-698, 1986.

[55] OpenCV. Open Source Computer Vision v2.4.3 documentation: feature detection. http://docs.opencv.org/modules/imgproc/doc/feature_detection.html, 2012. Accessed October 29, 2012.